Verification of the Bragg Scatter Method on the WSR-88D

Joshua G. Gebauer[1,2], Jeffrey G. Cunningham[3], W. David Zittel[3], Robert R. Lee[3]

[1]*National Weather Center Research Experience for Undergraduates*

Norman, Oklahoma

[2]*California University of Pennsylvania*

California, Pennsylvania

[3]*Radar Operations Center Application Branch*

Norman, Oklahoma

ABSTRACT

For the purpose of radar quantitative precipitation estimates, differential reflectivity (Z_{DR}) plays a crucial role and must be accurately calibrated. Currently, some WSR-88Ds in the Next Generation Weather Radar (NEXRAD) fleet may have systematic Z_{DR} biases due to errors in the measurement of the H and V channels. The Radar Operations Center (ROC) monitors these systematic Z_{DR} biases by measuring returns from external targets that should produce or can be adjusted to zero decibels (dB). One such target that has an intrinsic Z_{DR} = 0 dB is Bragg scatter, a clear-air return caused by turbulent mixing in refractive index gradients. The ROC implemented a method the National Severe Storms Laboratory developed to detect Bragg scatter on the WSR-88D. This study uses atmospheric sounding data as truth to verify the radar based Bragg scatter detection method from January to June 2014 (11,521 radar/sounding pairs). Measurements of refractivity gradients and Richardson number from the 00Z sounding (indicators of conditions conducive to Bragg scatter) are compared to radar-based method detections between 00Z and 02Z. Sounding analyses reveal that the potential for Bragg scatter occurs 95.43% of radar/sounding pairs at vertical layers below 5 km in the continental United States (CONUS). However, due to the method's strict data filters and volume coverage pattern (VCP) requirements, the method only detects Bragg scatter 4.03% of the time (464 radar/sounding pairs). Of the 464 pairs, Bragg scatter detection is verified 84.7% of the time at the same height indicated by the sounding. Climate region characteristics influence variability of verification statistics. We expect that improvements to the data filters for Bragg scatter detection, better use of available VCPs, and improved scanning techniques will increase frequency of Bragg scatter detection.

1. Introduction

Radar-based quantitative precipitation estimates (QPE) require accurate radar system calibration. Recently, the United States upgraded the Next Generation Weather Radar (NEXRAD) network to dual-polarization capability. With the upgrade, the network's Weather Surveillance Radars - 1988 Doppler (WSR-88Ds) began measuring and reporting dual-polarization variables, to include: differential reflectivity (Z_{DR}), correlation coefficient (ρ_{hv}), and differential phase (ϕ_{dp}). These new variables are useful for identifying hydrometeor class, distinguishing meteorological versus non-meteorological targets, and improving QPE performance. Z_{DR} represents the ratio of the horizontal and vertical return power and provides insight into the shape and size of the hydrometeors and is a significant factor in current QPE equations; however, WSR-88D Z_{DR} measurements may have a systematic bias caused by the radar system hardware (Ice et al., submitted 2014).

The Radar Operations Center (ROC) monitors systematic WSR-88D Z_{DR} biases by collecting hydrometeor target data during operational scans. System biases are detected when the Z_{DR} values of light precipitation and dry snow targets deviate systematically from expected Z_{DR} values. Recently, the ROC began using clear air returns in addition to hydrometeors to monitor systematic Z_{DR} bias (Hoban et al. 2013). The clear air returns, caused by Bragg scattering, could possibly provide more accurate systematic Z_{DR} bias estimates since Bragg scatter has an intrinsic Z_{DR} of 0 dB (Melnikov et al. 2011). The ROC Bragg scatter detection method is unique and has

Corresponding Author: Joshua G. Gebauer, California University of Pennsylvania, 250 University Ave California, PA
e-mail: geb6699@calu.edu

yet to be verified quantitatively. This study accomplishes that goal and strives to improve the understanding of the physical characteristics of Bragg scatter.

2. Bragg Scatter

Bragg scatter is clear-air backscatter caused by turbulent mixing in a layer of the atmosphere with large magnitude refractive index gradients (Melnikov et al. 2011). The reflectivity caused by Bragg scatter is proportional to the refractive index structure parameter C_n^2 using the equation (Otterstan 1969a; Doviak and Zrnic 2006),

$$\eta = 0.38\lambda^{-1/3}C_n^2 \qquad (1)$$

where η is the reflectivity and λ is the wavelength of the radar. The value for C_n^2 can be obtained from equation (11.143) from Doviak and Zrnic (2006),

$$C_n^2 = a^2\varepsilon^{-1/3}K_\phi \times 10^{-12}\left(\frac{d\phi}{dz}\right)^2 \qquad (2)$$

where a is a dimensionless constant, ε is the rate at which turbulent energy per mass is dissipated, K_ϕ is the coefficient of turbulent diffusion, and ϕ is the potential refractive index. Otterstan (1969b) demonstrated that for the scales at which the potential refractive index gradients occur for Bragg scatter, it is necessary that the reference height is the layer at which the scattering is taking place. Also, equation 2 is only valid if there is turbulence in the layer of interest.

In order for Bragg scatter to be detected by radar, the turbulent eddies must occur at scales that are half the radar wavelength, which for NEXRAD radars is 5 cm. Melnikov et al. (2011) examined the polarimetric qualities of Bragg scatter and determined the intrinsic Z_{DR} = 0 dB. This occurs because the turbulence that causes Bragg scatter is isotropic. The refractive index gradients, which are a primary contributor of the strength of the reflectivity returns, occur due to changes in pressure, temperature, and humidity with height (Rinehart 2010; Davison et al. 2013b). These gradients often occur at the top of the convective boundary layer; the location where most Bragg scatter was detected by Melnikov et al. (2011). Figure 1 shows an example of a Bragg scatter from KLIX which is a WSR-88D in Slidell, LA. Bragg scatter is typically seen in radar bins that form a ring around the radar at ranges of 10 to 80 km, which have a Z < 10 dBZ, ρ_{hv} > 0.98, uniform ϕ_{dp}, and Z_{DR} ≈ 0 (Melnikov et al. 2011; Cunningham et al. 2013).

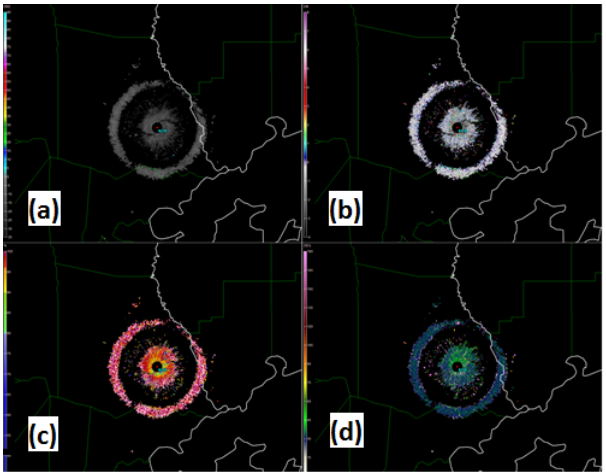

FIG. 1. An example of Bragg scattering from KLIX in New Orleans, LA on 01-05-2014 at 00:08:25 Z. a) Reflectivity (dBZ), b) Differential reflectivity (dB), c) Correlation coefficient, d) Differential phase (deg)

Bragg scatter may be an excellent external target with which to estimate Z_{DR} bias on the NEXRAD fleet because Bragg scatter is not necessarily limited to specific climate regions and should occur year-round. Attempts have been made to determine the average value of C_n^2 which could be used as an indicator of the frequency of Bragg scatter. Gossard (1977) calculated C_n^2 with height in different air masses and found that C_n^2 decreases more rapidly with height in continental air masses than maritime air masses. This may indicate that Bragg scatter might be harder to detect with radar in continental air masses. Other studies have also tried to find an average value of C_n^2, but the results have been too variable to arrive at a definitive number (Doviak and Zrnic 2006). The scientific literature is silent regarding the frequency of Bragg scatter detection with the NEXRAD network.

3. Bragg Scatter Method

The purpose of the Bragg scatter method is to identify Bragg scatter cases to estimate systematic Z_{DR} bias in the WSR-88D fleet. The method works by filtering out radar bins that do not have the base variable and dual polarization properties of Bragg scatter. The remaining bins must meet additional statistical criteria, such as bin count, distribution spread, and number of

volumes, to make a Bragg scatter method identified case. Some Bragg scattering events are not identified as cases because the case will not provide a useful bias estimate.

A brief overview of the Bragg scatter method will be presented here. For a more detailed description see Hoban et al. (2013). First, the method will only attempt to identify Bragg scatter when there are eight consecutive volume coverage patterns (VCP) in either 32 or 21. VCP 32 is a clear air mode, while VCP 21 is often used when precipitation is far from the radar. A range of 10-80 km and elevations from 2.4° to 4.5° are used to ensure that ground clutter is being omitted. The radar bins are then passed through additional filters which are shown in Table 1. The Z_{DR} for the bins that pass the data filters are compiled into a histogram for statistical testing. If the total number of radar bins from cases that contribute to the histogram is less than 10,000, the cases are excluded due to poor sampling. The interquartile range (IQR), the difference between the 75th and 25th percentiles of the histogram, must be less than 0.9 dB as cases contaminated with clutter or biota have broadened histograms since ground clutter and biota tend to have high Z_{DR} values. The final test is a precipitation filter that was not included in the Hoban et al. (2013) design and was added later by the ROC. Like the Z_{DR} histogram, a reflectivity histogram is generated. If the 90th percentile of reflectivity values of the range filtered data is greater than -3 dBZ, then the case is assumed to be contaminated with precipitation and is not used to estimate the Z_{DR} bias. If the case passes the three statistical filters, the case is classified as Bragg scatter. The bias is then determined by finding the difference the mode of the distribution of Z_{DR} values is from zero decibels.

TABLE 1. The data filters used in the Bragg scatter method developed by Hoban et al. (2013).

Variable	**Filter Value**
VCP:	32, 21
Elevations:	Between 2.4º and 5.0°
Range:	10 to 80 km
Correlation coefficient:	> 0.98 & < 1.05
Reflectivity:	< 10 dBZ
Signal to noise ratio:	-5 to 15 dB
Velocity:	> |2| ms^{-1}
Spectrum Width:	> 0 ms^{-1}

Initial testing of the Bragg scatter method has identified problems with the detection of Bragg scatter on some occasions. Specifically, a Z_{DR} bias estimate will be identified as an outlier that is different from the running trend of the bias estimates. The outliers are normally biased toward the positive values. This indicates the Bragg scatter method is misidentifying cases that are contaminated with non-Bragg scatterers and providing inaccurate bias estimates. Also, initial investigations revealed a lower frequency of detection of Bragg scatter in certain geographical regions. In the eastern continental United States (CONUS), Bragg scatter was detected more frequently than the western CONUS. When Bragg was detected in the west, the quality of the cases was typically poor, particularly in the mountain regions. Since the initial testing only looked at 17-19Z, it is hypothesized that the initial testing was not representative of the peak Bragg scatter time for the western CONUS, and the conditions that are conducive to Bragg still do occur in these regions.

4. Methods

a. Refractivity Gradients

A visual study of Bragg scatter cases that were identified with the method was conducted to gain an understanding of the characteristics of Bragg scatter observable on radar. In addition to the radar fields, the corresponding atmospheric soundings were examined. During the study, it was found that the temperature and dew point profiles from soundings often indicated cases when Bragg scatter occurred on the radar. Atmospheric layers with inversely correlated temperature and dew point profiles often produce large index of refraction discontinuities. Equation 2 shows that these gradients contribute proportionally to C_n^2. The index of refraction is related to refractivity by the equation:

$$N = (n-1)\times 10^6 \qquad (3)$$

where N is the refractivity and n is the index of refraction. The refractivity gradients can be calculated by using a differential version of Equation 3 from Davison et al. (2013),

$$\frac{\Delta N}{\Delta Z} = 77.6\frac{1}{T}\frac{\Delta p}{\Delta z} - \left(77p - 5.6Se_s + 7.5\times10^5\frac{Se_s}{T}\right)\frac{1}{T^2}\frac{\Delta T}{\Delta Z} + \left(-5.6 + 3.75\times10^5\frac{1}{T}\right)\frac{S}{T}\frac{\Delta e_s}{\Delta z} + \left(-5.6 + 3.75\times10^5\frac{1}{T}\right)\frac{e_s}{T}\frac{\Delta S}{\Delta z} \quad (4)$$

where T is the temperature; p is the pressure in millibars; S is the saturation ratio; and e_s is the saturation vapor pressure in millibars.

The 00Z sounding was linearly interpolated to create more layers for the refractivity gradient calculation. The refractivity gradient was then calculated using Equation 4, where Δz = 50 m. The average magnitude of refractivity gradients that Bragg scatter layers normally occur in was determined to create a critical value to identify potential Bragg scatter layers in the refractivity profile. This value was calculated from soundings where there was a clear visual indication that Bragg scatter was occurring and no other contamination was present. The refractivity gradient magnitudes that occurred in Bragg layers were compiled into a histogram and this histogram was compared to a histogram of refractivity gradient magnitudes that were associated with non-Bragg layers. This revealed Bragg layers often have refractivity gradients of magnitude greater than 0.05 m^{-1} while non-Bragg layers rarely had gradients of such magnitude. However, the 0.05 m^{-1} magnitude may not be consistent for all times of the year. To ensure non-Bragg cases are not identified, a buffer was added to the 0.05 m^{-1} value, so that only gradients with a magnitude larger than 0.07 m^{-1} are considered a potential Bragg layer.

b. Richardson number

The refractivity gradient test alone was not sufficient for the verification of the Bragg scatter method. Large scale turbulent layers were identified as another method for finding Bragg scatter layers because turbulent mixing can generate refractivity gradients. This dynamical situation can be illustrated with another equation for C_n^2 (equation 11.149a from Doviak and Zrnic 2006),

$$C_n^2 = \frac{a^2\varepsilon^{2/3}TR_f}{(1-R_f)g\dfrac{d\theta}{dz}}\left(\frac{K_\phi}{K_H}\right)\times10^{-12}\left(\frac{d\phi}{dz}\right)^2 \quad (5)$$

where R_f is the Richardson number, and K_H is the diffusion coefficient of heat. One can assume a threshold value of $C_n^2 = C_1$ is needed to cause Bragg scattering for a particular radar. If a hypothetical layer of the atmosphere is experiencing turbulence, but $C_n^2 < C_1$, then the radar will not initially detect Bragg scatter. As time continues, the turbulence in this layer will increase the refractivity gradients at the top and bottom of the turbulent layer due to an increase in temperature and humidity gradients at the top and bottom of the layer (Davison et al. 2013). This mixing would also cause the static stability of the top and bottom of the turbulent layer to increase. If ε, T, R_f, K_ϕ, K_H are held constant, the threshold value of C_n^2 can now be attained if the refractivity gradients that are created increase more quickly than the static stability. This type of change in the refractivity gradient can only occur if there is a significant contribution to the gradient by humidity. These refractivity gradients that develop can occur on scales that the interpolated sounding cannot identify, which provides an explanation to why the refractivity test was not sufficient. Therefore, turbulence needed to be included in the verification scheme. These layers of turbulence were identified by calculating the Richardson number every 50 m using,

$$Ri = \frac{N^2}{\dfrac{\Delta u^2}{\Delta z} - \dfrac{\Delta v^2}{\Delta z}} \quad (6)$$

and N is the Brunt-Vaisalla frequency,

$$N = \sqrt{\frac{g}{\theta_v}\frac{\Delta\theta_v}{\Delta z}} \quad (7)$$

where θ_v is the virtual potential temperature. The Richardson number can be used to determine the stability of the atmosphere as a function of temperature and wind shear. When the Richardson number is less than 0.25, Kelvin-Helmoltz instability can occur. This instability type has the ability to generate turbulence (Markowski and Richardson 2010). Therefore, a layer with a value less than or equal to 0.25 was considered a turbulent layer capable of creating Bragg scatter layers.

The Richardson number will not provide an absolute confirmation of Bragg cases identified by radar because not all turbulent layers are able to create refractivity gradients strong enough for Bragg scattering. The Richardson number identified layer should be considered as a condition conducive to Bragg scattering, but not sufficient. Some caution should then be used when using the Richardson number statistics.

c. Verification Scheme

The Bragg scatter method was run for January through June 2014 for 66 CONUS NEXRAD radars that were within 100 km of a sounding site to identify Bragg scatter cases that occurred from 00Z to 02Z (Fig. 2). This time period was chosen so the 00Z sounding would be representative of the atmosphere during the time the Bragg scatter method was run. For the purpose of this study, a height estimate was added to the Bragg scatter method. This height calculation estimated the height of each radar bin that passed the data filters using the equation,

$$H = \sqrt{r^2 + (k_e a)^2 + 2rk_e a \sin\theta_e} - k_e a + h_r \quad (8)$$

where, r is range, k_e is a constant equal to 4/3, a is the radius of the Earth, Θ_e is angle of elevation, and h_r is height of the radar surface (Doviak and Zrnic, 2006). After the bin heights were referenced to sea level, they were compiled into a histogram of 50 m intervals. The distribution of Bragg scatter bin heights can then be compared to the calculated refractivity gradients and Richardson number for the corresponding 00Z sounding.

FIG. 2. Map of the WSR-88D radars used in this study. The outlined regions are the NCDC climate regions.

The classification of the different case types is separated into radar detected cases and radar undetected cases. A radar detected case is a day in which Bragg scatter is identified by the radar during the 00Z-02Z time period, while a radar undetected case occurs when Bragg scattering was not detected during the same time period. The two case types are further classified using the following classification scheme (Fig. 3):

1) RADAR DETECTED CASES

The major mode of the distribution of Bragg scatter bin heights was found and then compared to the refractivity gradient profile of the corresponding sounding. If the refractivity gradient profile identified a potential Bragg layer using the criteria described in 4a, and this layer occurred at the mode of the distribution of Bragg scatter bin heights ± 250 m, then the case was classified as a "refractivity hit" (Fig. 4). If the case did not satisfy the refractivity gradient test, the distribution of bin heights were compared to the Richardson number profile of the corresponding sounding. If the Richardson number profile identified a potential Bragg layer using the criteria described in 4b, and this layer occurred at the mode of the distribution of Bragg scatter bin heights ± 250 m (Fig. 5), then the case was classified as a "Richardson hit". If the case does not pass the Richardson number test, then the case was classified as "no explanation".

2) RADAR UNDETECTED CASES

Radar undetected cases are classified solely on the sounding data. If the refractivity gradient profile had a potential Bragg layer that was identified using criteria described in 4a below 5000 m, then the case was classified as a "refractivity miss". If the refractivity gradient profile did not indicate Bragg, the analysis then moves to the Richardson number test. Any potential Bragg layer indicated by the Richardson number using criteria described in 4b below 5000 m caused the case to be classified as a "Richardson miss". A case that did not satisfy either testing criteria was classified as a "correct null".

The verification of the Bragg scatter method was done using contingency table statistics shown in Table 2. The contingency table is set up in this fashion due to the

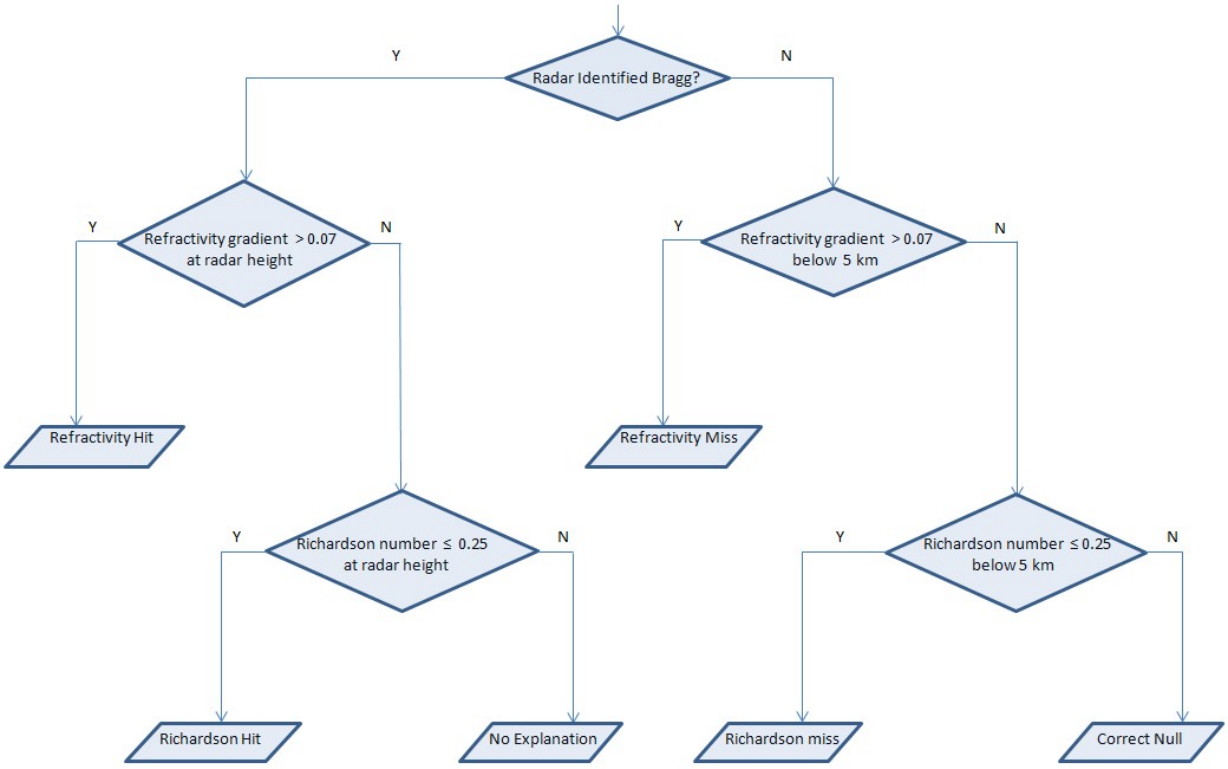

FIG. 3. Flow chart of the classification scheme use to classify cases.

varying confidence levels of the different types of cases. Confirmation of Bragg scatter using refractivity gradients has less uncertainty because the gradients directly contribute to the magnitude of C_n^2. Richardson number confirmation, however, is less certain as turbulence, on the scale which the Richardson number is able to be calculated on the sounding, is a creator of refractivity gradients and does not contribute to C_n^2 directly. Another way of thinking is that the refractivity gradients cases are cases in which there is a high likelihood that Bragg scatter is occurring, while Richardson number cases are cases where conditions are conducive to Bragg scatter occurring, but not always sufficient for Bragg scatter to be visible on radar.

TABLE 2. The example contingency table used for Bragg verification

	Bragg Detected		**Bragg Not Detected**	
Sounding Indicates Bragg	Refractivity Case Hit (ReH)	Richardson Case Hit (RiH)	Refractivity Case Miss (ReM)	Richardson Case Miss (RiM)
Sounding Doesn't Indicate Bragg	No Explanation (NE)		Correct Null (CN)	

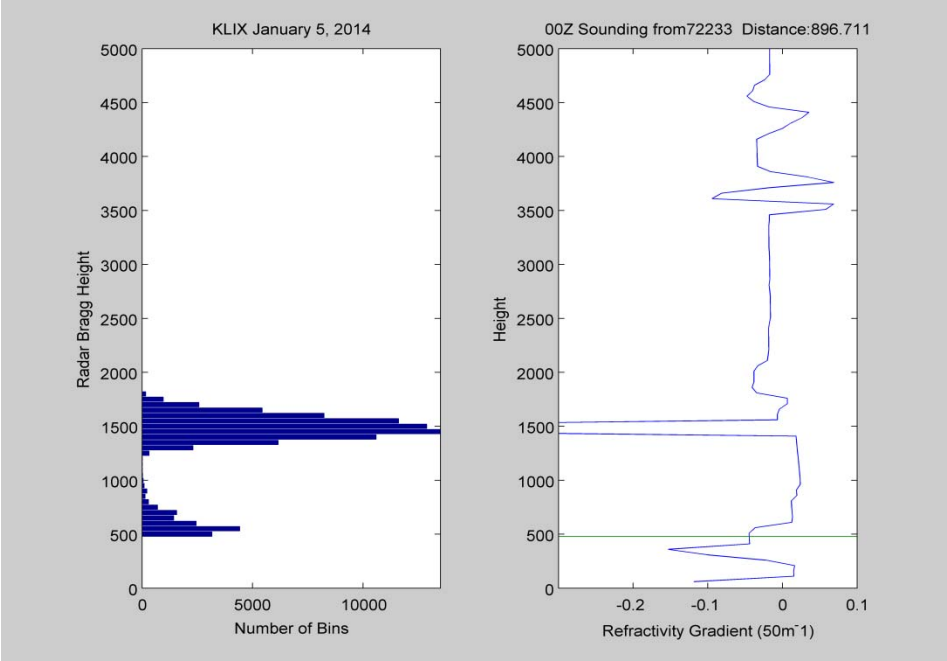

FIG 4. The refractivity gradient and distribution of bin heights for the case shown in Figure 1. This case would be classified as refractivity hit since the mode of the distribution of bin heights matches a refractivity gradient magnitude maximum.

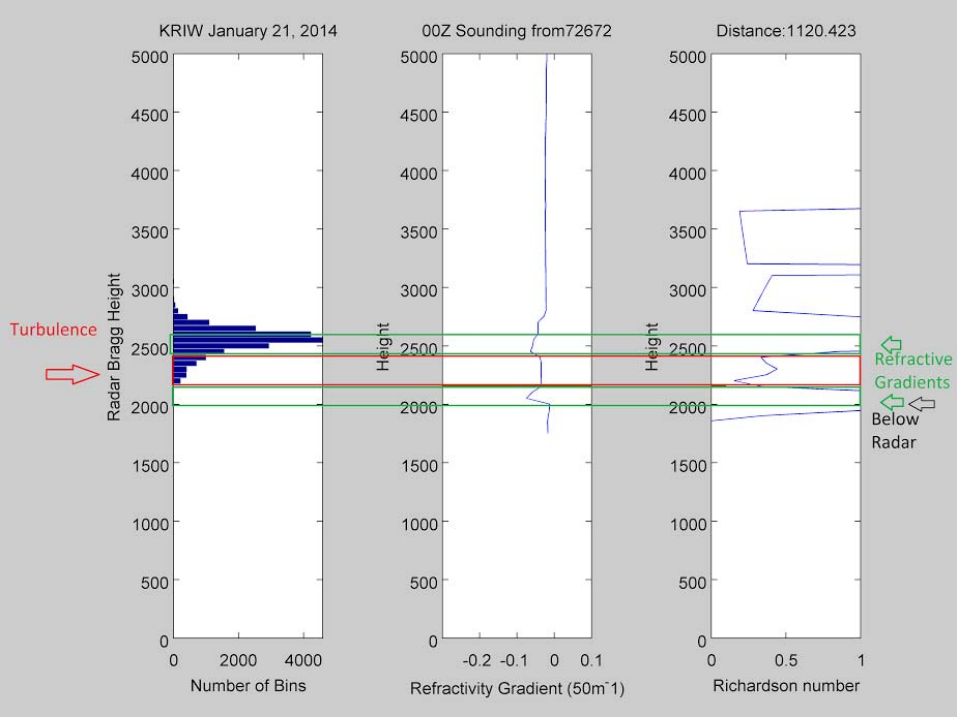

FIG. 5.Case from KRIW on January 21, 2014. An example of a turbulent layer creating refractivity gradients at the top and bottom of the layer. The radar detected bin heights occur in one of these refractivity layers, however, this layer would not be confirmed by the refractivity test, but is confirmed by the Richardson test

5. Results and Discussion

Table 3 shows the results of the total cases in a contingency table format. The Bragg scatter method is detecting sounding confirmed Bragg scatter that can be used for Z_{DR} bias estimates 3.41% of cases, while the method misses 92.02% of cases where conditions are conducive to Bragg scattering. These two percentages together show that soundings indicate that Bragg scattering could potentially occur in 95.43% of cases examined. The primary cause of missed cases is that the radar is not in the correct VCP which occurs in 43% of the total cases.

Missed cases can also be caused by biota, precipitation, and other contaminates that causes a case of Bragg scattering to fail the statistical filters. This means a missed case could actually have visually detectable Bragg; however, these types of cases would not provide good estimates of Z_{DR} biases. Therefore, for the purposes of the ROC, missed cases can actually be an indicator that the method is performing well.

Lastly, the possibility exists that Richardson number test is overestimating the occurrence of Bragg scatter as layers that meet the critical Richardson number are common in the atmosphere. Whether or not these turbulent layers develop into Bragg scatter layers has a strong dependence on moisture. When looking at radar detected cases, however, the Richardson test has some more validity since the range tested is limited to the area the radar observes Bragg scattering.

TABLE 3. The results of the total number of cases (11521) examined by the Bragg scatter method in the contingency table format shown in Table 2. The number of cases that are in each classification are in parentheses.

N = 11521	**Bragg Detected**		**Bragg Not Detected**	
Sounding Indicates Bragg	2.10% (242)	1.31% (151)	61.77% (7116)	30.25% (3485)
Sounding Doesn't Indicate Bragg	0.62% (71)		3.96% (456)	

The percentages of refractivity hits and misses and Richardson hits and misses for each National Climatic Data Center (NCDC) climate region are shown in Figure 6 and 7. The total percentages of refractivity cases (hits and misses) generally decreases from east to west, with the maximum percentage of cases occurring in the southeast and the minimum percentage of cases occurring in the southwest. This correlates well with the distribution of moisture in these regions which should be expected given the dependency of refractivity gradients on humidity. In areas where there are large numbers of refractivity cases, the Richardson number cases (Fig. 7) are expected to be low since most of the cases can be explained by refractivity gradients, for which there is higher confidence. However, the sites that have low refractivity cases (Fig. 6) do experience high percentages of Richardson cases. The large percentage of correct null cases (Fig. 8) in the west indicates that overall the conditions conducive to Bragg scattering occur less frequently in these areas. The three maps together (Fig. 6, Fig. 7, Fig. 8) show that Bragg scatter has the possibility to occur over the entire CONUS, with the most confidence in Bragg scattering occurring in the southeast with decreased confidence towards the west and north.

An important statistic on the overall performance of the Bragg scatter method is the "no explanation" cases. In these cases, the method identifies the case as Bragg scatter, but there is no potential Bragg layer seen on the sounding at the distribution of bin heights. "No explanation" cases occur in 0.62% of the total cases (Table 3). The percentage of "no explanation" cases by NCDC climate region is shown in Figure 9. The outlier estimations of Z_{DR} biases are most likely caused by these "no explanation" cases. These cases occur when meteorological scatter has similar properties to Bragg scatter except for Z_{DR}. This allows the meteorological scatter to pass the data filters and contaminate the bias estimate. Often, the meteorological scatter that is incorrectly identified is dry snow or drizzle since these scatterers have polarimetric properties similar to Bragg scatter.

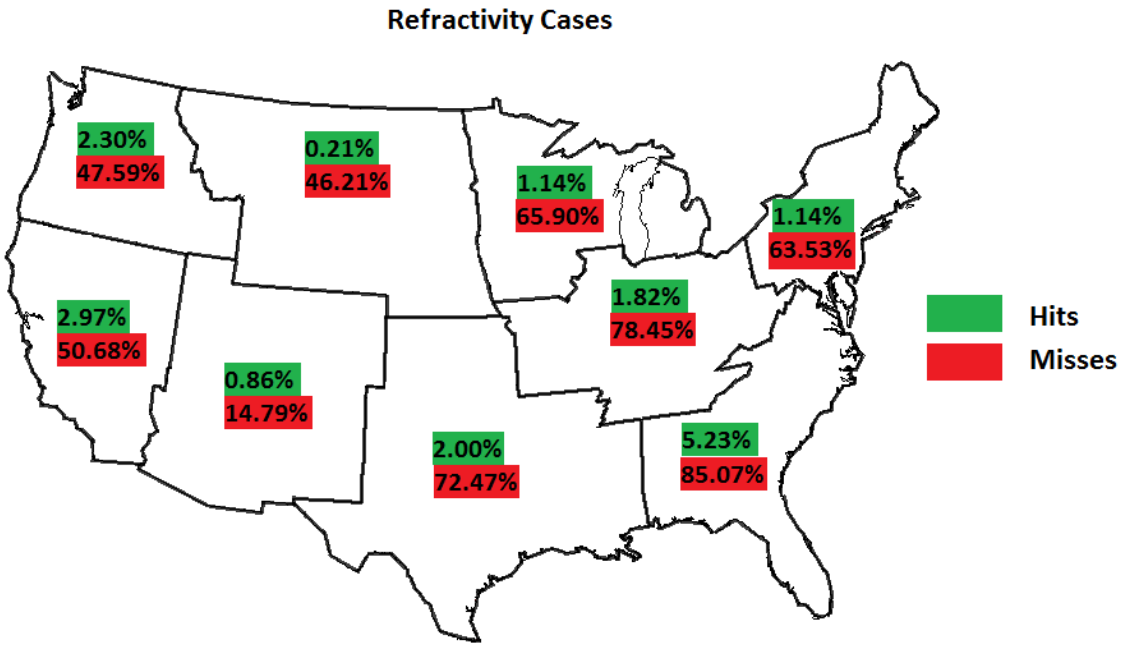

FIG. 6. The percentage of refractivity hits and misses for each NCDC climate region.

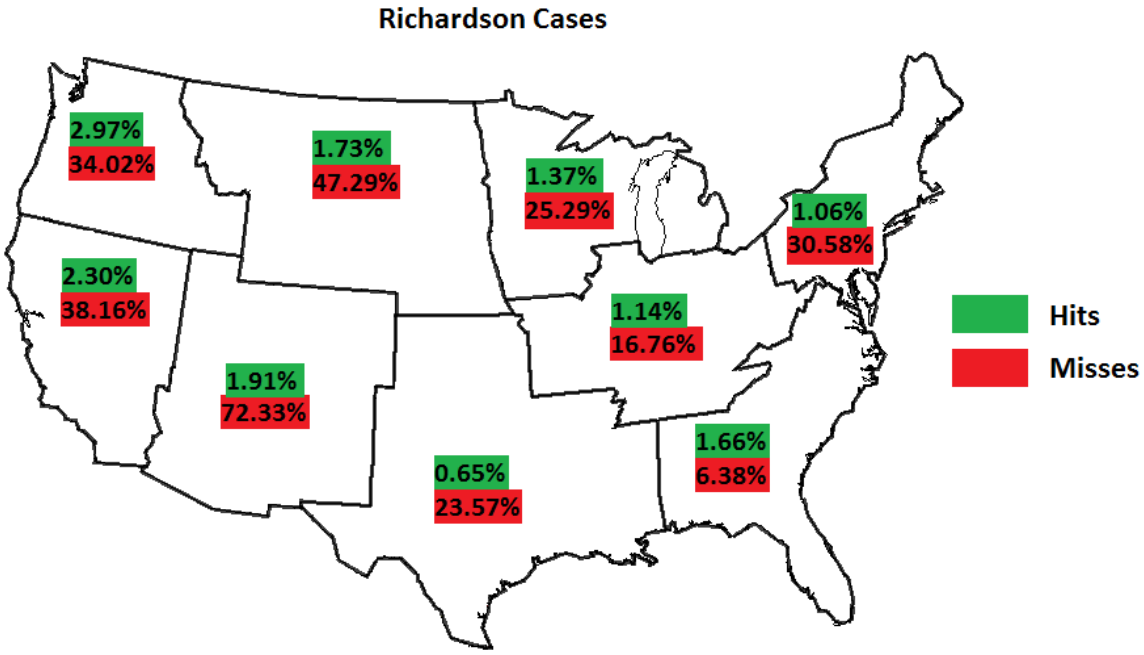

FIG. 7. The percentage of Richardson hits and misses for each NCDC climate region.

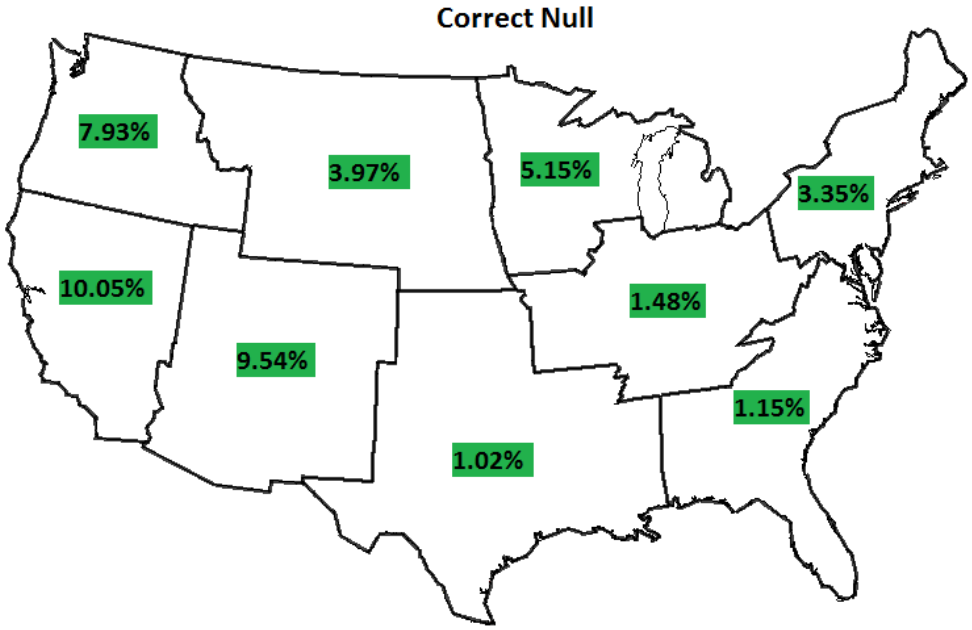

FIG. 8. The percentage of correct null cases for each NCDC climate region.

Not all “no explanation” cases, however, produce outlier Z_{DR} estimates. This indicates that Bragg scatter is actually occurring in some of these cases. The reason this may occur is because of dynamics of the critical Richardson number. When the critical Richardson number of 0.25 reached, turbulence will begin to develop. Once the turbulence has started, the flow can remain turbulent until the Richardson number becomes greater than 1 (Ottersten, 1969a). Therefore, some of the “no explanation” cases could be Bragg scatter that is occurring in one of these layers with a Richardson number > 0.25 and < 1.

The accuracy of the Bragg scatter detections can be evaluated by looking at just the radar identified cases**.** Of the 464 cases that are identified by the radar as Bragg scatter, 84.7% of the cases can be confirmed. The accuracy, however, varies by climate region. The analysis of just radar detected cases by NCDC climate region is shown in Figure 10 where the refractivity confirmed cases have the highest confidence that Bragg scatter is occurring. The Richardson confirmed cases have less confidence, but still provide a physical explanation for why Bragg scattering would be occurring. Lastly, the “no explanation” cases do not have a physical explanation for Bragg scattering in the identified layer based off of the sounding information, and therefore, cannot be confirmed. Adding together the percentage of refractivity hits and Richardson hits for a climate region will result in the estimated accuracy for that region. For every region, there is a higher amount of confirmed cases than not confirmed which proves that most of the time the Bragg scatter method is detecting correct cases. The method works the best in the southeast region with only 6.90% of the cases classified as “no explanation”; while in the east north central region 31.25% of cases are “no explanation” cases. Figure 8 also shows the highest confidence in the Bragg scatter method is in the southeast where most of the radar detected cases can be confirmed by the refractivity test. Generally, confidence decreases towards the west and north where more cases need to be confirmed by the Richardson test.

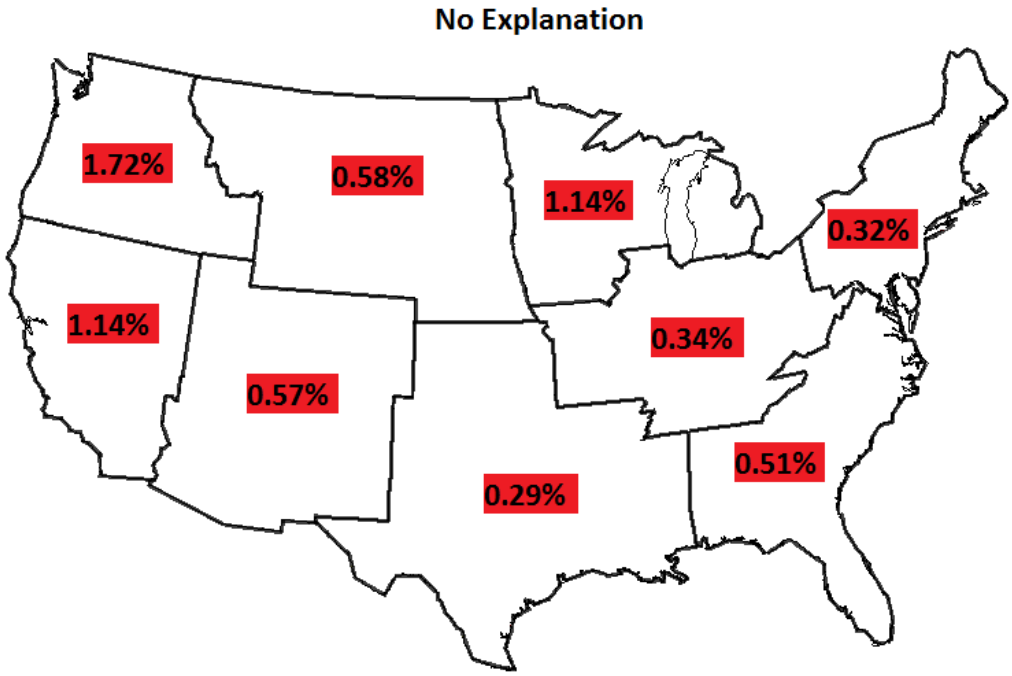

FIG. 9. The percentage of “no explanation” cases for each NCDC climate region.

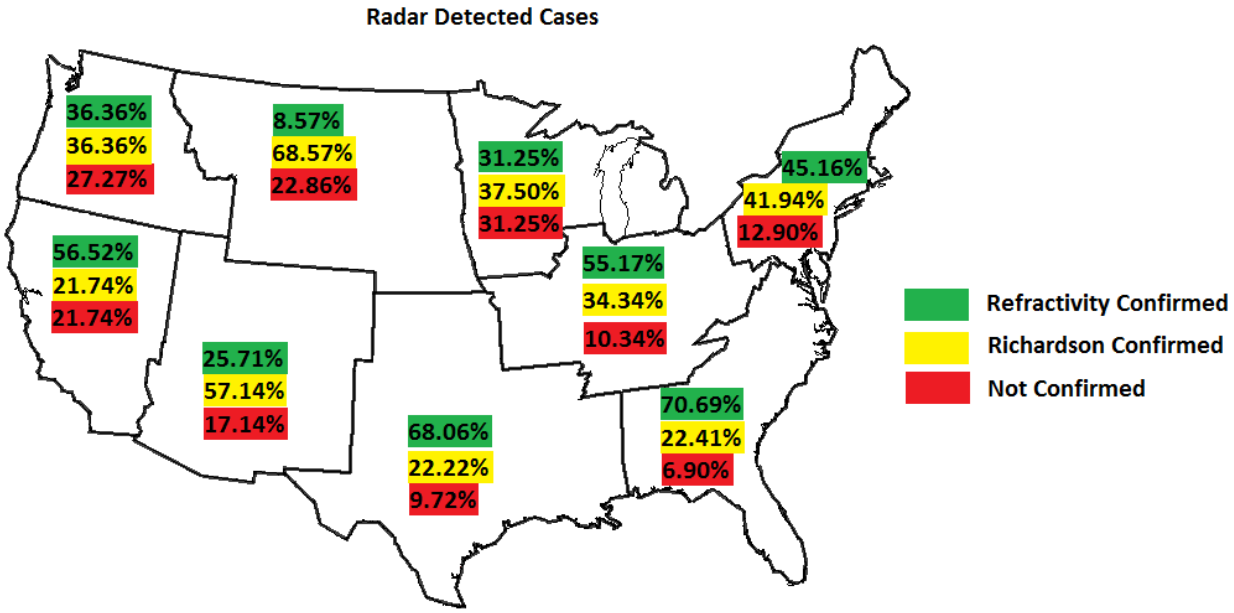

FIG. 10. Percentage of refractivity hits, Richardson hits, and “no explanation” cases for radar detected cases in each NCDC climate region. The different shading of numbers represents the confidence that Bragg scatter is occurring. Green – high, Yellow – medium, Red – none.

Dry snow and drizzle can frequently occur in the climate regions with higher values of "no explanation" cases during certain times of the year. This could possibly explain the higher number of unconfirmed cases in these regions. Future studies should verify the method by month to test this hypothesis.

6. Conclusions

This study developed a quantitative verification scheme using sounding data for the Bragg scatter method for the WSR-88D radar. The verification scheme is limited on absolute accuracy due to the small scales at which Bragg scatter can be seen by the WSR-88D, but provides a conservative estimate on the performance of the Bragg scatter method. This verification scheme also uses varying levels of confidence when giving the performance estimate. The verification was done by grouping radars into NCDC climate regions. This approach produced several interesting conclusions.

1) Radar detected Bragg cases verify in the majority of detections for every NCDC climate region (84.7%). However, there is less confidence in the performance of the Bragg scatter method in the western and northern CONUS. This reduced confidence correlates well with areas of the country that have low average moisture amounts.
2) Misidentifications are more likely to occur in the western and northern CONUS. This conclusion is aligned with what initial visual verification found. More studies are needed to determine the exact cause of the higher misidentifications in these regions.
3) Soundings indicate that conditions conducive to Bragg scattering are common (95.43% of cases) with decreasing regularity in regions with less moisture. However, even in the regions with less moisture Bragg scatter still occurs frequently. Therefore, the possibility exists that the Bragg scatter method could be improved to detect more cases. With more detections, the Bragg scatter method may be used for more meteorological applications, such as boundary layer height estimates, and turbulence strength measurements.

Overall, this verification proved the Bragg scatter method can be useful for the entire CONUS; however, the accuracy of the method varies by climate region. Therefore, future attempts at improving the Bragg scatter method should focus on incorporating the idiosyncrasies of Bragg scatter in the regions with less accuracy.

7. Acknowledgements

Special thanks to Daphne LaDue and the National Weather Center Research Experience for Undergraduates for their support in this research. This material is based on work supported by the National Science Foundation under Grant No. AGS-1062932.

8. References

Cunningham, J. G., W. D. Zittel, R. R. Lee, R. L. Ice, and N.P. Hoban, 2013: Methods for identifying systematic differential reflectivity (Z_{DR}) biases on the operational WSR-88D network. *36th Conf. on Radar Meteorology*.

Davison, J. L., R. M. Rauber, L. D. Girolamo, 2013: A revised conceptual model of the tropical marine boundary layer. Part II: detecting relative humidity layers using Bragg scattering from S-band radar. *J. Atmos. Sci*., **55**, 3025-3046.

Doviak, R. J., and D.S. Zrnic, 2006: *Doppler Radar and Weather Observations.* 2nd ed. Dover Publications, 562 pp.

Gossard, E. E., 1977: Refractive index varience and its height distribution in different air masses. Radio Science, **12**, 89-105.

Hoben N. P., J. G. Cunningham, W. D. Zittel, 2013: Using Bragg scatter to estimate systematic differential reflectivity biases on operational WSR-88Ds. *Real-world Research Experience for Undergraduates at the National Weather Center*.

Hoben, N. P., J. G. Cunningham, W. D. Zittel, 2014: Using Bragg scatter to estimate systematic differential reflectivity biases on operational WSR-88Ds. *30th Conference on Environmental Information Processing Technologies*, Atlanta, GA. Amer. Meteor. Soc.

Ice, R. L., A. K., Heck, J. G. Cunningham, W. D. Zittel, submitted 2014: Challenges of Polarimetric Weather Radar Calibration. *8th European Conference on Radar in Meteorology and Hydrology*, Garmisch-Partenkirchen, Germany.

Markowski P., and Y. Richardson, 2010: *Mesoscale Meteorology in Midlatitudes.* Wiley-Blackwell, 407 pp.

Melnikov, V. M., R. J. Doviak, D.S. Zrnic, and D.J. Stensrud, 2011: Mapping Bragg scatter with a polarimetric WSR-88D. *J. Atmos. Oceanic Technol.*, **28**, 1273-1285.

Ottersten, H., 1969a: Atmospheric structure and radar backscattering in clear air. *Radio Science.,* **4**, 1179-1193.

Ottersten, H., 1969b: Mean vertical gradient of potential refractive index in turbulent mixing and radar detection of CAT. *Radio Science.,* **4**, 1247-1249.

Rinehart, R. E., 2010: *Radar for Meteorologists*. 5th ed. Rinehart Publications.